



IAEA

INTERNATIONAL ATOMIC ENERGY AGENCY

22nd IAEA Fusion Energy Conference

Geneva, Switzerland, 13-18 October 2008

IAEA-CN-165/ EX/P6-1

Filament dynamics and transport in the Scrape-Off-Layer of ASDEX Upgrade

A. Herrmann, A. Schmid, H.W. Müller, M. Maraschek, J. Neuhauser, A. Kirk¹,
ASDEX Upgrade Team

Max-Planck-Institut für Plasmaphysik, Boltzmannstr. 2, D-85748 Garching, Germany
¹EURATOM/UKAEA Fusion Association, Culham Science Centre, Abingdon, UK

This is a preprint of a paper intended for presentation at a scientific meeting. Because of the provisional nature of its content and since changes of substance or detail may have to be made before publication, the preprint is made available on the understanding that it will not be cited in the literature or in any way be reproduced in its present form. The views expressed and the statements made remain the responsibility of the named author(s); the views do not necessarily reflect those of the government of the designating Member State(s) or of the designating organization(s). In particular, neither the IAEA nor any other organization or body sponsoring this meeting can be held responsible for any material reproduced in this preprint.

Filament dynamics and transport in the Scrape-Off-Layer of ASDEX Upgrade

A. Herrmann, A. Schmid, H.W. Müller, M. Maraschek, J. Neuhauser, A. Kirk¹,
ASDEX Upgrade Team

Max-Planck-Institut für Plasmaphysik, Boltzmannstr. 2, D-85748 Garching, Germany
¹EURATOM/UKAEA Fusion Association, Culham Science Centre, Abingdon, UK

e-mail: albrecht.herrmann@ipp.mpg.de

Abstract Measurements at different experiments have shown that a few 10% of the energy loss from the confined plasma during an ELM cycle is deposited to non-divertor components. Usually, these components are not designed to receive high heat loads. The measurement and the extrapolation of these non-divertor loads to a next step fusion reactor are essential for the design of in-vessel components. The energy released from the pedestal plasma during an ELM is concentrated in field aligned helical structures, so called filaments, distributed around the torus with a quasi mode number in the order of 10. These filaments are rotating and moving radially. Theoretical modelling of the filament dynamics relies on different assumptions and results in contradictory predictions for the velocity and size scaling of such filaments. This paper reports on measurements of velocity, radial extend, and electron density of filaments in the far SOL of ASDEX Upgrade, as well as on the energy content of such filaments by a new filament probe. The probe carries a set of radially and poloidally separated Langmuir pins around a magnetic pick-up coil and can be moved towards the plasma by a magnetic drive. Radial and poloidal velocity of filaments are calculated from time delay measurements together with the amplitude and width of the corresponding ion saturation current signal. 466 filaments have been analysed. Several trends have been derived from a series of scatter plots. Most important, it has been shown that filaments with large radial extent move faster than smaller ones, and that filaments with higher density move faster than filaments with less density. From a comparison of filament size and density, we could show that the filaments loose density by parallel losses and broaden radially with time. In AUG, the filaments would be depleted after a distance of about 12 cm from the separatrix. The radial velocity of filaments does not seem to vary with time or distance from the separatrix, i.e. no acceleration could be identified from the data. The data would favour models that predict large filaments to move faster. The modelling of the magnetic signal requires the assumption of a rotating mode structure inside the separatrix otherwise the required currents are not consistent with the measured ion saturation currents. From the comparable decay length of heat load and particle flux a simple one point model for the ion energy and heat load is derived.

1. Introduction

Measurements at different experiments have shown that a few 10% of the energy loss from the pedestal plasma during an ELM cycle is deposited to non-divertor components [1]. Usually, these components are not designed to receive high local heat loads. The measurement and the extrapolation of these non-divertor loads to a next step fusion reactor are essential for the design of in-vessel components. The energy released from the pedestal plasma during an ELM is concentrated in field aligned helical structures, so called filaments, distributed around the torus with a quasi mode number in the order of 10 [2-4].

These filaments are rotating and moving radially. Theoretical models of the filament dynamics relies on a variety of assumptions and results in partly contradictory predictions for the velocity and size scaling of such filaments [5-7].

This paper reports on measurements of filament parameters by Langmuir probes, magnetic pick-up coils and IR-cameras in ASDEX Upgrade.

2. Experimental

The data discussed in this paper is based on localized measurements in the outer midplane of ASDEX Upgrade by a set of electric, magnetic and thermographic diagnostics. The probes are toroidally separated by about 20° but connected along magnetic fields as shown in Fig. 1.

A new filament probe to measure the filament dynamics at a given local position was installed in 2006 and updated for the 2007 campaign. The probe combines a magnetic pick-up coil measuring the radial component of the local magnetic field and Langmuir probes (LPs). The LPs are positioned in the tungsten coated graphite shielding of the pick-up coil. Radial and poloidal velocity of filaments are calculated from time delay between the maximum of the ion saturation current as measured by the radially and toroidally separated Langmuir pins (see Fig. 2).

A magnetic drive was developed and installed to change the radial position of the filament probe by about 5 cm [8]. This allows to move the probe out of the limiter shadow towards the plasma by about 1 cm. The radial dependence of the filament behaviour was scanned by moving the plasma with respect to the probe, varying the separatrix to probe distance between 5 and 11 centimetres. For the presented results, 466 filaments of type-I ELMs have been analysed from several discharges with the following parameters: $I_p = 0.8$ MA, $B_t = -2.5$ T, $P_{\text{heat}} = 6-7.5$ MW and a line averaged density $n = 6 \times 10^{19} \text{ m}^{-3}$.

In addition to the filament probe, a Mach type reciprocating probe was used to measure the ion saturation current in the far SOL outside any limiter shadow with 2 MHz sampling rate. Simultaneously, the surface temperature of the probe head was recorded by a high speed IR-camera [9] and the heat flux to the probe head was calculated with the 2D-code THEODOR [10]. The settings of the camera were optimized to get sufficient spatial resolution (2 mm) and a good time resolution of 100 $\mu\text{s}/\text{frame}$ in order to allow the detection of filaments during an ELM.

Inside the reciprocating probe head a 3D magnetic pick-up coil was used to measure the components of the magnetic field during ELMs.

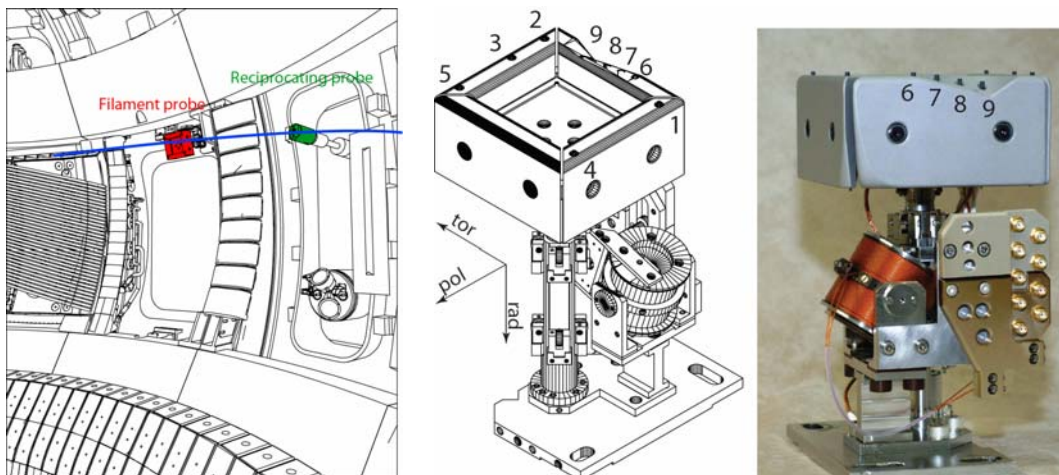


Fig. 1 (left) CAD view of one part of the ASDEX Upgrade vessel. The blue line shows the filament as a field aligned structure. The surface temperature of the reciprocating probe head was measured with a fast IR-camera. (middle and right) Probe head and magnetic drive of the filament probe. A magnetic pick-up coil in the center is surrounded with a tungsten covered graphite shield with embedded Langmuir probes, operated as single probes in ion current saturation branch. The numbering of the LPs is as used in the text. The Langmuir pins stick 5 mm out of the graphite tiles. For measurements, the filament probe is moved out of the limiter shadow by applying a voltage to the magnetic coil that is then tilted due to the torque caused by the external magnetic field.

From these plots, it can be concluded, that filaments with large radial extent move faster than smaller ones, and that filaments with higher density move faster than filaments with less density. This allows a verification of models and predictions for filament movement. Models that predict a decrease of the radial velocity with size and density can be excluded on the base of these data.

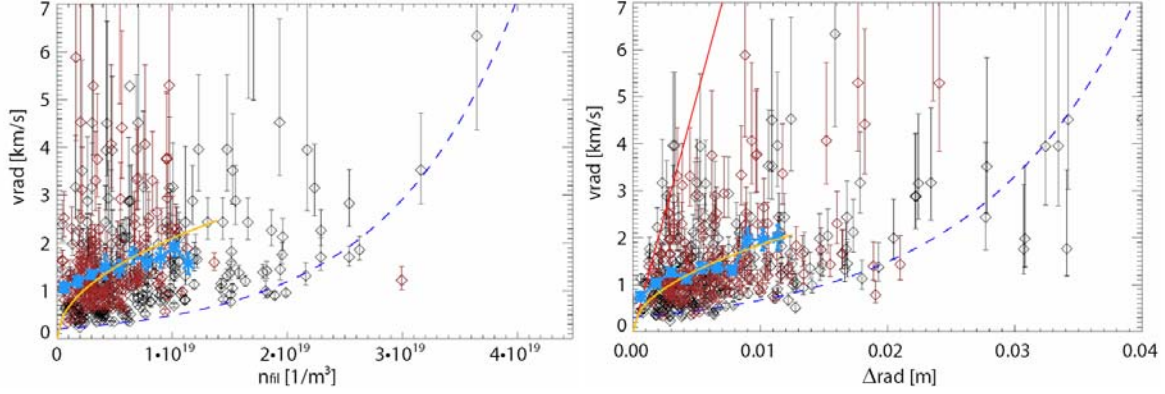


Fig. 3 Scatter plots of the radial filament velocity in dependence on the electron density (left) and the radial extent of the filament (right). The dashed blue curves show a lower limit for the radial velocity. Large or dense filaments move faster than smaller or thinner ones. Light blue: Mean radial velocity obtained by a boxcar averaging technique. Orange: Fits of to the mean radial velocities with a square root like dependence from the abscissa value. The red curve indicates the detection limit due to the sampling rate of the data acquisition system.

From the variation of the radial distance between separatrix and probe follows that the density of the filament decreases and the radial width increases with increasing distance. Whether or not this means that the total amount of particles is constant is investigated in Fig. 4 where the particle content of a filament is plotted vs. the radial distance. The dashed line is a linear fit with $n_{fil} \Delta_{rad} \leq 7 \cdot 10^{17} m^{-2} - 6.5 \cdot 10^{18} m^{-3} dR$. The solid curve is the product of the individual fits of n_{fil} and Δ_{rad} [11]. The slope of the dashed line is negative, which means that the particle content of a filament decreases from its initial value of about $n_{fil}^0 = 7 \cdot 10^{17} m^{-2}$ with time, i.e. with the distance from the separatrix, which can be explained by parallel losses. With the most likely radial velocity of $v_{rad} = 1 km/s$, the resulting loss rate is $6.5 \cdot 10^{22} / m^2 s$. This is in quite good agreement with a simple estimate for free particle flow along the field lines, $\Gamma = n_{fil} c_s = 1.3 \cdot 10^{23} / m^2 s$, using the most probable filament density and the sound speed for the temperatures of section 3.2.

In AUG, the filaments would be depleted after a distance of about 12 cm from the separatrix. The radial velocity of filaments does not seem to vary with time or distance from the separatrix, i.e. no acceleration could be identified from the data. Again, the data favour models that predict large filaments to move faster [12].

Plotting the data as probability distribution function (PDF) results in the following parameters for the radial dynamics of the filaments: $v_{rad} = 1.1 km/s$, $\Delta_{rad} = 2.7 mm$.

The same procedure as shown in Fig. 2 was applied to the pins 1-5 measuring the velocity perpendicular to the magnetic field lines. The relation between toroidal and poloidal movement is given by the local field inclination. This is for the presented geometry about $v_{pol}/v_{tor} = 1/5$. The deduced parameters for the poloidal movement are: $\Delta_{pol} = 1 cm$ with a broader velocity distribution $v_{pol} = 0.5-2.6 km/s$.

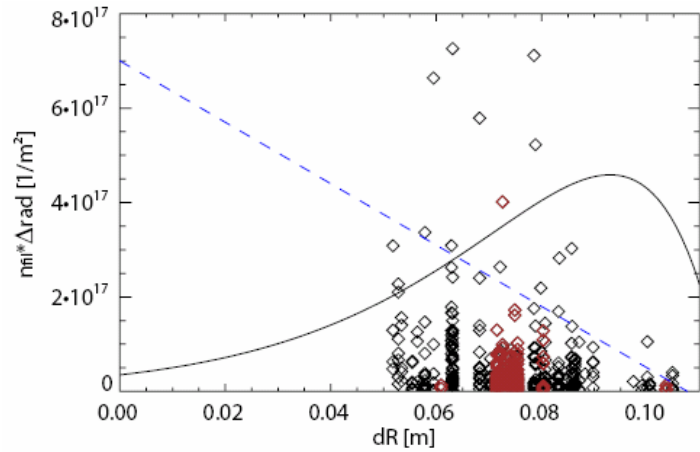


Fig. 4 Particle content of the filament in dependence of the radial distance between separatrix and filament probe. The dashed line shows a linear fit, the solid line the product of the individual fits of the density and radial size variation with radial distance.

3.2. Heat and particle flux

Combined measurements of heat and particle flux were done with both LPs in the field of view of the thermography system. A radial scan of far SOL parameters was performed by varying the radial distance between separatrix and probe position.

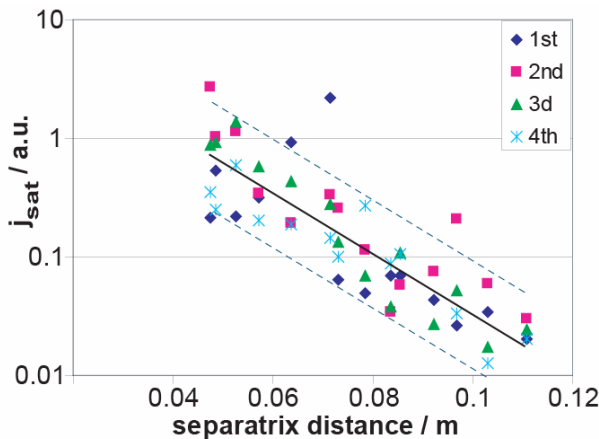


Fig. 5 Radial decay of the j_{sat} signal for the first 4 filaments in an ELM

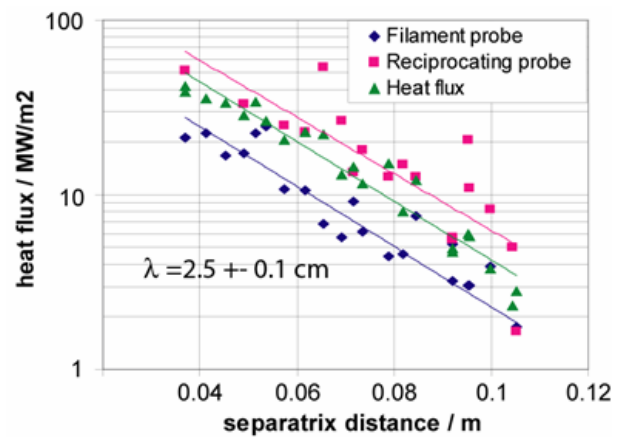


Fig. 6 Radial decay of the particle flux (j_{sat}) measured by the filament and the reciprocating probe and the heat load to the probe head of the reciprocating probe.

In Fig. 5 the radial decay of the first 4 filaments of an ELM are plotted. It is obvious that despite the large scatter of about a factor 10 the data points follow an exponential decay. In addition, there is no degradation of the filament strength with the temporal distance from the start of the ELM, at least for the first filaments of an ELM. This should be expected for quasi mode numbers of about 10. The reason for the strong scatter might be a variation of the starting parameters, i.e. the filament parameters in the pedestal region or a scatter of the radial velocity resulting in more or less time for parallel losses.

The radial decay of the j_{sat} signal measured by the filament and the reciprocating probe, respectively, and the heat load to the probe head of the reciprocating probe are shown in Fig. 6. For comparison, the particle flux is expressed in heat flux by using a distance independent factor of $\gamma_s T_e = 100 \text{ eV}$ as conversion factor, with γ_s the sheath transmission factor. The

radial decay of the ion saturation current and the heat load show comparable decay lengths. This is not trivial because heat and particle flux are linked by the particle temperature.

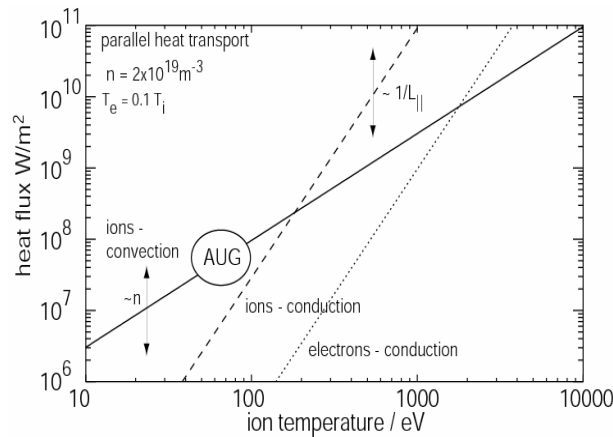


Fig. 7 Contribution of electron and ion heat conduction, as well as ion heat convection to the parallel energy loss in dependence on the temperature. For this plot a ratio of $T_i/T_e = 10$ is assumed.

Comparable decay lengths for heat and particle flux implies a constant temperature in the far SOL and an energy loss from the filament due to particle loss at the ends, i.e. dominating convective losses in a semi-collisional regime. This assumption is checked in Fig. 7 by plotting the main contributors to parallel energy loss, heat conduction by electrons and ions ($\sim T_{e,i}^{7/2}$), as well as ion convective losses ($\sim n_e T_i^{3/2}$). For smaller temperatures, convection becomes the dominant loss mechanism, but decreases with decreasing density. Typical parameters for a regime with dominating ion convection losses in ASDEX Upgrade are $T_i < 100 \text{ eV}$, $n_e \approx 1 \times 10^{19} \text{ m}^{-3}$ ($T_i/T_e > 2.6$). This is consistent with the experimental data for ion temperature and filament density calculated from heat and particle flux of $T_i = 30 \div 60 \text{ eV}$ and $n_e \approx 4 \div 6 \cdot 10^{19} \text{ m}^{-3}$.

3.3. Magnetic probe measurement

The pick-up coils in the filament and the reciprocating probe gives a total of 7 magnetic coils to measure the magnetic signature of a filament. The signals show a clear ELM signature as shown in Fig. 9. This magnetic signature was simulated by moving current distributions in front of the magnetic probes [12]. 3 cases and its parameter dependence were investigated: a uni- and a bi-directional current distribution in the far SOL near to the probe with motion parameters from the filament probe (filament case) and a bi-directional current distribution in the pedestal region with size and velocity as expected for rotating modes (mode case).

Bi-directional current distributions can be fitted with a unique parameter set to the measured magnetic signals for the 3D magnetic coils, i.e. the same fit parameter set is applied to simulate all 3 signals of the 3D magnetic probe. A bi-directional current distribution represents a filament where the current is short circuited in the filament itself and not across external structures. The effect of parameter variation on the shape of the magnetic signal is shown in Fig. 8.

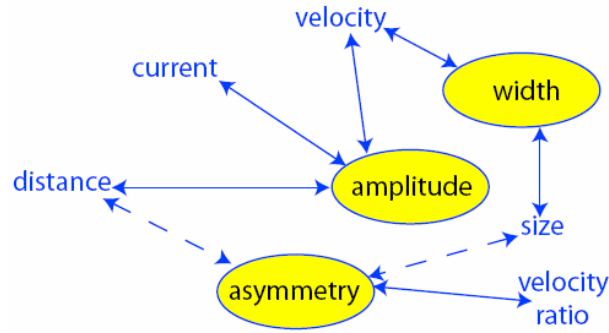


Fig. 8 Parameter dependencies for the determination of filament properties from the magnetic signature. Solid lines indicate strong influences, dashed lines denote weak dependencies. Multiple dependencies make the full determination difficult, but additional information can strongly reduce the parameter space.

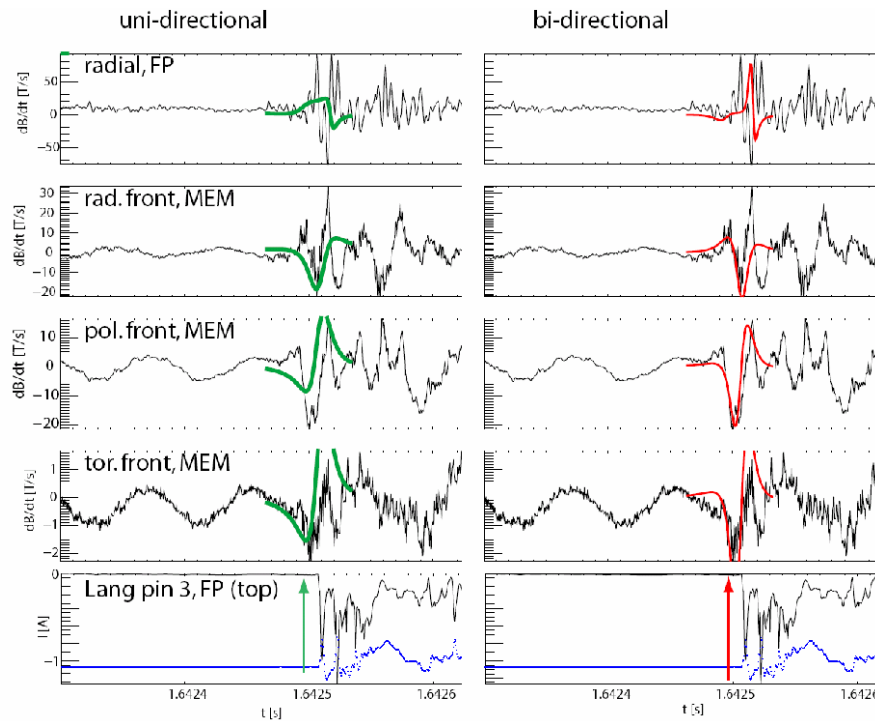


Fig. 9 Magnetic signature of the magnetic pick-up coils of the filament probe and the 3 components of a 3D coil at the reciprocating probe. (left) Matching the measurement with an uni-directional current with $I = 60\text{A}$. Right: Bi-directional current with $I = 150\text{A}$. Filament parameters: $\Delta_{rad}^* = 7\text{ mm}$, $\Delta_{pol}^* = 15\text{ mm}$, $v_{rad} = 2.2\text{ km/s}$, $v_{pol} = 3.2\text{ km/s}$. The arrow denotes the point where the filament touches pins 2 and 3 in the simulation (filament case).

The result of the simulation is shown in Fig. 9. The shape as well as the absolute signal can be well reproduced with a bi-directional current distribution for both, the filament and the mode case, respectively, a filament rotating slowly ($v_{pol} = 3.5\text{ km/s}$) in the SOL and a fast ($v_{pol} = 20\text{ km/s}$) rotating filament inside the separatrix. The required current densities are about 120 A/cm^2 for the filament in the far SOL and 600 A/cm^2 inside the separatrix, respectively. This parameters, required to simulate the measured magnetic signals, have to be compared to the maximum ion saturation current of about 15 A/cm^2 that was measured by Langmuir probes in the far SOL. I.e. the signal of the magnetic pick-up coils is caused by remote filaments of the pedestal region in contact to the core plasma allowing a high current flow.

4. Summary

Measurements in the far SOL at the outer midplane of ASDEX Upgrade by a set of electric, magnetic and thermographic diagnostics to characterize filament dynamics are presented. A new filament probe in ASDEX allow for the local measurement of ELM filament dynamics. A mean radial velocity of about 1 km/s with a radial extension of 3mm, a poloidal velocity between 0.5 and 2.6 km/s and 1 cm poloidal extend are deduced. The data favour models that predict large filaments to move faster.

A comparison of heat and particle decay reveals that the far SOL is in an energy transport regime where ion losses are dominant ($T_i = 30-60$ eV). Extrapolating such a regime to ITER would result in the following parameters for the ion temperature of $T_i < 400$ eV.

All deduced parameters of the filaments in the far SOL show a large scatter (up tot a factor of 10). This is due to a scatter of the starting parameters in the pedestal region and has to be investigated further. Furthermore, a local measurement in the far SOL detects filaments arising from different toroidal positions with different transition times in the SOL.

The measured magnetic ELM signature can be modelled with a bi-directional current distribution rotating both in the pedestal region and the far SOL. However, the required current density for a filament in the far SOL is an order of magnitude higher than the measured one so that the magnetic signal is assumed to be from filaments in the pedestal region.

5. References

- [1] HERRMANN, A., et al., "Power deposition outside the divertor in ASDEX Upgrade", *Plasma Phys. Control. Fusion* 46:971-979; 2004.
- [2] NEUHAUSER, J., et al., "Structure and dynamics of spontaneous and induced ELMs on ASDEX Upgrade", *Nucl. Fusion* 48; 2008.
- [3] EICH, T., et al., "Nonaxisymmetric energy deposition pattern on ASDEX upgrade divertor target plates during type-I edge-localized modes", *Phys. Rev. Lett.* 91; 2003.
- [4] KIRK, A., et al., "Structure of ELMs in MAST and the implications for energy deposition", *Plasma Phys. Control. Fusion* 47:315-333; 2005.
- [5] GARCIA, O. E., et al., "Computations of intermittent transport in scrape-off layer plasmas", *Phys. Rev. Lett.* 92; 2004.
- [6] D'IPPOLITO, D. A., et al., "Cross-field blob transport in tokamak scrape-off-layer plasmas", *Physics of Plasmas* 9:222-233; 2002.
- [7] KRASHENINNIKOV, S. I., "On scrape off layer plasma transport", *Physics Letters A* 283:368-370; 2001.
- [8] SCHMID, A., et al., "Magnetically driven filament probe", *Review of Scientific Instruments* 78; 2007.
- [9] "High speed CMT camera", www.thermosensorik.de.
- [10] HERRMANN, A., et al., "Limitations for Divertor Heat Flux Calculations of Fast Events in Tokamaks", *Europhysics Conference Abstracts (CD-ROM, Proc. of the 28th EPS Conference on Controlled Fusion and Plasma Physics, Madeira 2001)* 25A:2109-2112; 2001.
- [11] SCHMID, A., et al., "Experimental observation of the radial propagation of ELM induced filaments on ASDEX Upgrade", *Plasma Phys. Control. Fusion* 50; 2008.
- [12] SCHMID, A., "Characterization of Type-I ELM Induced Filaments in the FAR Scrape-Off Layer of ASDEX Upgrade", 10/35. Munich: Max-Planck-Institut für Plasmaphysik; 2008.